

Compensating for Drusen in Retinal Vessel Segmentation

Lei Zhang¹
Lei.zhang@uea.ac.uk

Mark Fisher¹
http://www2.cmp.uea.ac.uk/~mhf/

Wenjia Wang¹
Wenjia.Wang@uea.ac.uk

¹ School of Computing Sciences,
University of East Anglia, UK

Abstract

Segmenting vessels from retinal images, like segmentation in many other medical image domains, is a challenging task, as there is no unified way that can be adopted to extract the vessels accurately. This paper focuses on removing Drusen (isolated areas of brightness), a problem and a common source of error in automated vessel detection. We use the log-Gabor filter to calculate the local energy in the image and so identify the Drusen. A pre-processing stage comprising an average filter is then used to smooth the affected area in order to eliminate the imperfection before vessels are classified by an existing technique. The results confirm that the modified method shows some improvement compared to a previously published method when tested using the STARE database.

1 Introduction

In optometry, the appearance of blood vessels in the retina is an important indicator, which is routinely examined to detect diseases, including diabetes, hypertension, and glaucoma. For example, diabetic retinopathy (DR) is basically a main complication caused by diabetes, and it would lead to blindness if the diabetic patient did not receive the treatment in time. But the assessment of the retina is a skilled time consuming task [6], and as such it has been the focus of research into automatic assessment techniques. Amongst the methods or algorithms that have been presented, Echevarria and Miller [11] propose a method that utilizes the concept of level sets to remove the noise and a fast marching algorithm to trace the vessels. They also use a filter designed by Chaudhuri et al. [12] to enhance the image contrast. Farnell [4] presents a method that adopts a multi scale line operator (MSLO) filter to enhance the retinal blood vessels in the image and then implements Otsu's threshold selection approach [8] to segment the MSLO filter response. In [5] Diego Marín et al. adopts a neural network (NN) scheme and a 7-D vector comprising gray-level and moment invariant features is used for the pixel classification task. The general framework of blood vessel segmentation presented in [3] is similar to the above methods. Innovatively, Wu et al. [3] combines a diffusion enhancement Hessian-based, and matched filters, which incorporate edge constraints to produce a single

compound filter to enhance the image. This filter needs only one matched filter at each scale and is more efficient than other matched filters which require multiple filter applications per pixel [3]. Soares and Leandro *et al.* [7] proposed a scheme using the 2D Gabor wavelet to implement the noise filtering and vessels enhancement, then using a Bayesian classifier with class-conditional probability density functions named Gaussian mixture model (GMM) to identify whether pixels are vessel or not. Cinsdikici and Aydin [9] proposed a novel approach which is a hybrid model of matched filter (MF) and ant colony algorithm. The novel method overcomes an imperfection of classic MF that it improves the performance of detecting small branches of vessels (capillaries). Bob and Lin *et al.* [2] proposed a novel extension of the MF approach which is named MF-FDOG to distinguish the vessels from non-vessel step edges. The basis of MF-FDOG is that it detects the vessels objects by thresholding the retinal image's response to a zero-mean Gaussian function while using the local mean of the response to the first-order derivative of Gaussian (FDOG) to adjust the threshold level in order to remove the non-vessel edges. Although, many methods have been proposed and some success has been achieved, the algorithms frequently fail due to the challenging nature of retinal image analysis. The images are often contaminated by noise and suffer low contrast between the vessels and surrounding background. Cases in which suffer from existing damage due to disease can be particularly problematic and our work is focused in this area. In these pathologies local small brightness blobs especially located round vessels have the most important influences for segmentation. Hence, we aim to find what the brightness spots are and how we can reduce their affects for vessels segmentation.

1.1 Brightness area (Drusen)

Drusen (e.g. illustrated in the figure1) are deposits of epithelial cell waste that are located beneath the retina. They present as yellowish blobs which are brighter than the orange background, hence it appears more brightly in the green band of retinal images. This phenomenon may affect the accuracy of vessel segmentation which we found in the experiments (Fig. 2 b) and indicated in the other literatures [2][8]. Our scenario is that removing the brightness blobs (like Drusen) before implementing the segmentation in order to reduce the Drusen caused influences of vessel segmentation.

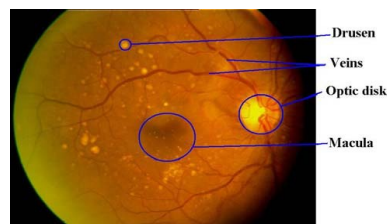


Figure 1 colour retinal image sample [13]

1.2 Materials

The experimental data, we choose from the STARE dataset which is publicly available on the website www.ces.clemson.edu/ahover/stare/. It's originally collected by Hoover *et al.* [1]. The images of dataset were stored as PPM format, 8 bits per colour channel and digitalized to size 700*605. The dataset contains two manual segmentations results made by 2 observers, and the first set of manual segmentation results is used as ground truth to evaluate the performances of two methods in our experiment.

2 Method

The framework of our method is primarily composed of four stages: 1. pre-processing, 2. Drusen detecting and removing, 3. using Matched filter to generate the maximal filter responses and 4. Convert the responses to binary by local entropy thresholding and using length filtering to remove the isolate objects.

2.1 Pre-processing

In pre-processing stage, we convert colour retinal images into gray level images by isolating the green channel, since other authors (e.g. Wu et al. [3]) have noted that contrast between vessels and background is enhanced in this channel. A two dimensional Gaussian filter is then adopted to remove the vessel reflection and smooth the image. From experiment experience we choose the parameters as $\sigma_x = 1.5$ $\sigma_y = 2$. At the end of pre-processing stage, we adjust the image to enhance the contrast between the vessels and background.

2.2 Drusen detection using local energy

A texture-based Drusen detection method [13] is adopted in our experiment, the texture of the drusen can be characterised in terms of local energy. The Local energy has been defined in [10] as the sum of squared responses of orthogonal pairs of Gabor or log-Gabor filters. Compared to Garbor filters, the log-Gabor filter has several advantages. It allows larger bandwidths to be efficiently implemented (typically 1 to 3 octaves), which in turn allows one to capture more features [13]. A log-Gabor filter can be expressed as

$$G(f, \theta) = \exp\left\{\frac{-[\log(f/f_o)]}{2[\log(\sigma_f/f_o)]}\right\} \times \exp\left\{\frac{-[\theta - \theta_o]}{2\sigma_\theta^2}\right\} \quad (1)$$

Where the former part of formula is radial component and the latter part is orientational component. f_o is the central radial frequency, θ_o is the filter direction. σ_θ , which defines the angular bandwidths, and σ_f represent the radial bandwidth which is computed by both σ_f and f_o . The local energy at every pixel(x,y) is calculated by summing squares of even and odd symmetric log-Gabor filter responses at every point (x,y). It is obtained as

$$E_{\theta_o}^{f_o}(x, y) = (R_{\theta_o}^{f_o, even}(x, y))^2 + (R_{\theta_o}^{f_o, odd}(x, y))^2 \quad (2)$$

Where $R_{\theta_o}^{f_o, even}(x, y)$ and $R_{\theta_o}^{f_o, odd}(x, y)$ present the responses of even and odd symmetric log-Gabor filters respectively. An example of the energy map is illustrated in Fig. 2 (c). The brighter areas of the image indicate higher values of local energy.

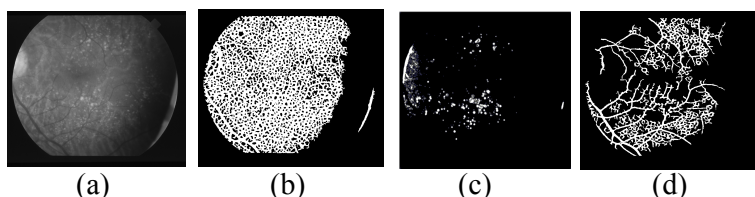


Figure 2 drusen detection and results, (a) is gray level image (b) segmented result using method [14] (c) binary drusen mask (d) segmented result using our modified method

Once Drusen detected they are removed by an averaging filter applied to the areas identified by the local energy map. We choose a filter size of 40×40 , and before apply the filter on the objective areas of image (the Drusen areas), we transform the local energy map to a binary image which is used to determine the range of averaging area. In our experiment, these areas, actually, are Drusen. The threshold is simply chosen by calculating the average value of energy map.

2.3 Matched filter

In [14] the authors adopt a 2-D Gaussian filter kernel with 12 different orientations. The vessel can be regarded as typical line feature with different orientations in the retinal image, and it may be oriented at any angle, hence, as noted in [14], we should implement filter kernels that can be rotated and aligned in any direction. In our experiment, we applied a set of 12 orientations ($0^\circ, 15^\circ, 30^\circ, 45^\circ, 60^\circ, 75^\circ, 90^\circ, 105^\circ, 120^\circ, 135^\circ, 150^\circ, 165^\circ$) of Gaussian kernel with one scale ($\sigma = 1.75$). The size of each Gaussian kernel is 16×15 pixels. Fig. 3 illustrated the Gaussian kernel with 12 different orientations. The enhanced image then is generated by taking the maximum filter responses at each pixel.

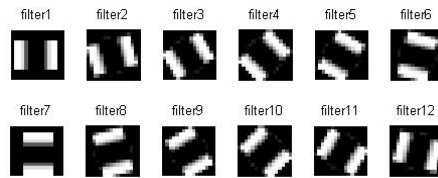


Figure 3 Gaussian kernels with 12 different orientations.

2.4 Segmentation method

Considering dependences of intensities between each image pixel, we follow the same approach to Chanwimaluang *et al.* [14] and take into account the spatial distribution of gray level. The segmentation method is composed of two steps. Firstly, we use a local entropy thresholding algorithm to compute the optimal threshold for classifying vessels and background. The second step is using length filtering to remove the isolate objects that may be misclassified. The primary task in local entropy thresholding is that of choosing parameters for the calculation of entropy. An optimal threshold is chosen based on the maximum of sum of second derivative entropies on different gray levels.

3 Experiment results

The parameters of method are trained on images which don't have manual segmentation result (ground truth), the test and evaluation procedure are applied on 18 STARE images for both original method proposed by Chanwimaluang *et al.* [14] and our improved method. We use standard measures of performance, namely, sensitivity ($TP/TP+FN$), specificity ($TN/TN+FN$) and accuracy ($TP+TN/TP+FP+TN+FN$). The sensitivity and specificity are the factors which indicate success rate of classifying vessel and non-vessel structures, respectively. The sensitivity is also known as TPF which represents the ratio of the number of correctly classified vessel pixels to the number of total vessel pixels in the ground truth. The accuracy indicates the ratio of total well classified pixels. In addition, the

algorithm's performance was also measured with receiver operating characteristic (ROC) curves. The ROC curves for each image are obtained by manually thresholding the image with the threshold values starting from 0 to 1 in a step of 0.01 (e.g. Fig. 4). The areas under the ROC curves for both original method and our method are listed in Table 1. Az indicates the area under the ROC curves, also is known as AUC. Columns indicated by 1 and 2 are our modified method and Chanwimaluang et al. [14] method, respectively. The last row of Table 1 shows the average sensitivity, specificity and accuracy values.

| Image | Sensitivity | | Specificity | | Accuracy | | Az | |
|----------------|-----------------|-----------------|---------------|---------------|---------------|---------------|---------------|---------------|
| | 1 | 2 | 1 | 2 | 1 | 2 | 1 | 2 |
| Im0001 | 0.700938 | 0.66857 | 0.9509 | 0.9279 | 0.9310 | 0.9072 | 0.9081 | 0.8926 |
| Im0002 | 0.738628 | 0.725829 | 0.9200 | 0.9001 | 0.9080 | 0.8885 | 0.9152 | 0.9065 |
| Im0003 | 0.769185 | 0.763385 | 0.9016 | 0.8957 | 0.8937 | 0.8878 | 0.9136 | 0.9112 |
| Im0004 | 0.534416 | 0.574709 | 0.9840 | 0.9809 | 0.9507 | 0.9508 | 0.9273 | 0.9181 |
| Im0005 | 0.582482 | 0.614554 | 0.9729 | 0.9672 | 0.9377 | 0.9354 | 0.9323 | 0.9347 |
| Im0044 | 0.690704 | 0.861405 | 0.9736 | 0.9112 | 0.9539 | 0.8204 | 0.9166 | 0.9406 |
| Im0077 | 0.766949 | 0.804131 | 0.9637 | 0.9526 | 0.9479 | 0.9407 | 0.9314 | 0.9261 |
| Im0081 | 0.824229 | 0.86459 | 0.9517 | 0.9382 | 0.9422 | 0.9327 | 0.9410 | 0.9346 |
| Im0082 | 0.726719 | 0.792195 | 0.9766 | 0.9634 | 0.9569 | 0.9500 | 0.9331 | 0.9330 |
| Im0139 | 0.708283 | 0.765393 | 0.9744 | 0.9465 | 0.9530 | 0.9320 | 0.9267 | 0.9275 |
| Im0162 | 0.717064 | 0.75338 | 0.9721 | 0.9600 | 0.9539 | 0.9453 | 0.9492 | 0.9488 |
| Im0163 | 0.745046 | 0.81283 | 0.9819 | 0.9669 | 0.9636 | 0.9549 | 0.9544 | 0.9519 |
| Im0235 | 0.795867 | 0.81401 | 0.9495 | 0.9440 | 0.9358 | 0.9325 | 0.9239 | 0.9235 |
| Im0236 | 0.697211 | 0.839155 | 0.9736 | 0.9310 | 0.9485 | 0.9227 | 0.9370 | 0.9366 |
| Im0240 | 0.663206 | 0.739102 | 0.9679 | 0.9577 | 0.9367 | 0.9354 | 0.9264 | 0.9187 |
| Im0255 | 0.720708 | 0.807852 | 0.9743 | 0.9584 | 0.9516 | 0.9449 | 0.9478 | 0.9474 |
| Im0291 | 0.74232 | 0.772621 | 0.9817 | 0.9769 | 0.9696 | 0.9666 | 0.9576 | 0.9518 |
| Im0319 | 0.747767 | 0.564538 | 0.9644 | 0.9851 | 0.9550 | 0.9670 | 0.9160 | 0.9107 |
| Average | 0.7151 | 0.7521 | 0.9630 | 0.9480 | 0.9439 | 0.9286 | 0.9310 | 0.9286 |

Table 1 Performance results on STARE data by both our method and Chanwimaluang et al. [14]. Considering the sensitivity, Specificity and Accuracy with ROC curve, we can say that the modified method improves the segmentation performance compared to original method, particularly reduce the miss-segmentation rate (FPF) that the rate of tissue not belong to vessel are miss-segmented as vessels. Observing from the Fig. 4, in contrast to original method's plus (+symbols) points line, we can find that the red point curve is closer to the top left corner.

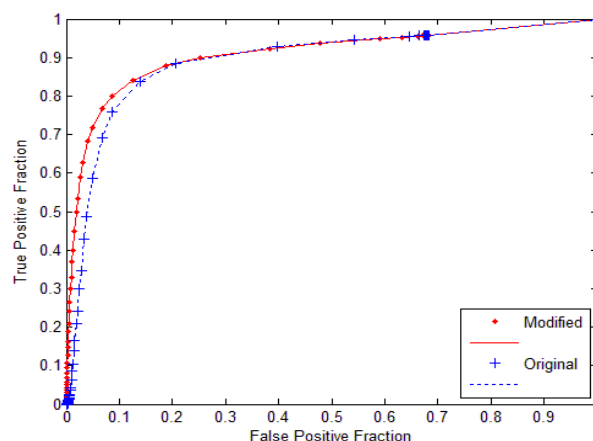


Figure 4 ROC curves for the first image of STARE

This confirms our method achieves some success in reducing the effects caused by Drusen which present as light spots in the image and produce false positives.

4 Conclusion

In this paper, we explored a method for extracting the vessel structure from retinal images. We use a log-Gabor filter to detect Drusen that produce bright areas in the image that can

produce errors in the vessel segmentation quality. Considering our experimental results (the sensitivity 0.7151, specificity 0.9630 and accuracy 0.9439 with AUC area under the ROC curve 0.9310) compare with original method (sensitivity 0.7521, specificity 0.9480 and accuracy 0.9286 with AUC area under the ROC curve 0.9286) we can say that the modified method improves the segmentation performance compare to original method, particularly reduce the miss-segmentation rate (FPF) that the rate of tissue not belong to vessel are miss-segmented as vessels. We can conclude that the additional step makes a valuable contribution and a significant improvement.

References

- [1] A. Hoover, *et al.*, "Locating blood vessels in retinal images by piecewise threshold probing of a matched filter response", *IEEE Trans. Med. Imaging* 19 (3) 203–210, 2000
- [2] Bob Zhang, *et al.*, "Retinal vessel extraction by matched filter with first-order derivative of Gaussian", *Computers in Biology and Medicine*, 40(4), 438-445, 2010
- [3] Changhua Wu, *et al.*, "A general framework for vessel segmentation in retinal images", In *Proceedings of CIRA*. 37-42, 2007.
- [4] D.J.J. Farnell, "Initial Results of an Automatic Blood-Vessel Segmentation Procedure in Digital Fundus Photographs via Multiscale Line Operators and Global Threshold Selection." 2009. <http://dirweb.king.ac.uk/miua2009/pdfs/miua/017.pdf>
- [5] Diego Marín, *et. Al.*, "A New Supervised Method for Blood Vessel Segmentation in Retinal Images by Using Gray-Level and Moment Invariants-Based Features", *Medical Imaging, IEEE Transactions on*, Volume:30, 146 – 158, 2011.
- [6] H. Schneiderman, *The Fundusoscopic Examination*, <http://www.ncbi.nlm.nih.gov/books/NBK221/>, 1990.
- [7] J. V. B. Soares, *et al.*, "Retinal vessel segmentation using the 2D Gabor wavelet and supervised classification," *IEEE Trans. Med. Imag.*, vol. 25, no. 9, 1214–1222, 2006.
- [8] L. Gang, O. Chutatape, and S. Krishnan, "Detection and measurement of retinal vessels in fundus images using amplitude modified second-order Gaussian filter," *IEEE Trans. Biomed. Eng.*, vol. 49, no. 2, 168–172, 2002.
- [9] M. Cinsdikici and D. Aydin, "Detection of blood vessels in ophthalmoscope images using MF/ant (matched filter/ant colony) algorithm", *Comput. Methods and Programs Biomed.* 96, 85–95. 2009.
- [10] M.C. Morrone and R. Owens, "Feature detection from local energy", *Pattern Recognition Letters* 1 103–113. 1987.
- [11] P. Echevarria T. Miller J. O'Meara, *Blood Vessel Segmentation in Retinal Images* February 8, 2004. http://robots.stanford.edu/cs223b04/project_reports/P14.pdf
- [12] S. Chaudhuri, *et al.*, "Detection of blood vessels in retinal images using two-dimensional matched filters". *IEEE Trans. on Medical Imaging*, 8(3):263-269, 1989.
- [13] S. Garg, J. Sivaswamy and G. D. Joshi, "Automatic Drusen Detection from colour retina", <http://cvit.iit.ac.in/papers/saurabh06Automatic.pdf>
- [14] T. Chanwimaluang and Guoliang Fan. "An efficient algorithm for extraction of anatomical structures in retinal images", In *Proc. of ICIP* (1), 1093-1096, 2003
- [15] T. Kurita, N. Otsu and N. Abdelmalik. "Maximum likelihood thresholding based on population mixture models," *Pattern Recognition* 25, pp. 1231–1240, 1992.